Attosecond Localization of Electrons in Molecules

ANDRÉ D. BANDRAUK,* STEPHANE CHELKOWSKI, HONG SHON NGUYEN

Laboratoire de Chimie Théorique, Faculté des Sciences, Université de Sherbrooke, Sherbrooke, Québec, J1K 2R1, Canada

Received 27 February 2004; accepted 26 May 2004
Published online 10 September 2004 in Wiley InterScience (www.interscience.wiley.com).
DOI 10.1002/qua.20252

ABSTRACT: Numerical solutions of the time-dependent Schrödinger equation for a 1D model non-Born–Oppenheimer H_2^+ are used to illustrate the nonlinear nonperturbative response of molecules to intense ($I \geq 10^{13}$ W/cm^2), ultrashort ($t < 10$ fs) laser pulses. Molecular high-order harmonic generation (MHOHG) is shown to be an example of such response and the resulting nonlinear photon emission spectrum is shown to lead to the synthesis of single *attosecond* (10^{-18} s) pulses. Application of such ultrashort pulses to the H_2^+ system results in localized electron wavepackets whose motion can be detected by asymmetry in the photoelectron spectrum generated by a subsequent probe attosecond pulse, thus leading to measurement of electron motion in molecules on the attosecond time scale. Int J Quantum Chem 100: 834–844, 2004

Key words: attosecond science; electron localization

1. Introduction

Advances in current laser technology allow experimentalists access to new laser sources for examining molecular structure and dynamics on the natural time scales for atomic (vibrational) motion, femtosecond (fs = 10^{-15} s). These new sources are ultrashort ($t_p \leq 10$ fs) and intense ($I \geq 10^{14}$ W/cm^2) [1]. Such pulses lead to a new regime of laser matter interaction, the nonlinear, nonperturbative regime. Thus, because the atomic unit (au) of electric field strength $E_0 = e/a_0^2 = 5 \times 10^9$ V/cm ($a_0 = 1$ au = 0.0529 nm) corresponds to an au of intensity $I_0 = cE_0^2/8\pi = 3.5 \times 10^{16}$ W/cm^2, laser intensities approaching I_0 have led to the discovery of new nonlinear phenomena in laser-atom experimental and theoretical studies [2], such as ATI (above threshold ionization) the multiphoton equivalent of single-photon photoionization; and HOHG (high-order harmonic generation) [3].

The study of interactions of intense ultrashort laser pulses with molecules is a relatively new science [4], with the first discovery of nonlinear nonperturbative laser-molecule interaction leading to a new concept,

Correspondence to: A. Bandrauk; e-mail: Andre.bandrauk@USherbrooke.ca

*Canada Research Chair in Computational Chemistry and Photonics

laser-induced molecular potentials (LIMPs)—predicted as early as 1981 [5] and recently confirmed experimentally [6, 7]. At the very high intensities now available, $I \geq 10^{14}$ W/cm^2, one now must consider dissociative ionization so that one must deal with bound–continuum transitions both in the electronic and nuclear Hilbert space. Multiphoton nonperturbative transitions in the nonlinear Hilbert space describing photodissociation only via LIMPs can be treated adequately, using a coupled equations approach based on the dressed molecule representation [4]. Inclusion of ionization involves treating numerically the complete field-electron-nuclear non-Born–Oppenheimer problem. This has been exactly solved recently for the 1D H_2^+ system [8], leading to the first calculation of nonlinear molecular photoelectronic spectra or ATI [9] and the concomitant Coulomb explosion (CE) spectra [10, 11]. This benchmark calculation has led to a new method of measuring nuclear wave functions by laser Coulombs explosion imaging (LCEI) [10, 11].

Electronic interaction with radiation in molecules differs from that of atoms because of the large delocalization of electrons in the former. As early as 1939, Mulliker [12] explained intense absorption bands due to large transition moments in molecules. Thus, in H_2^+, the electronic transition moment between the HOMO, $1\sigma_g$, and LUMO, $1\sigma_u$, $\mu(R) = \langle 1\sigma_g|z|1\sigma_u\rangle = R/2$, which leads to large nonperturbative radiative interactions at large distances, $V(R) = RE/2$, in a field of strength E. As an example, 1 au of field strength leads to 1 au = 27.2 eV of radiative interaction at the equilibrium distance $R \simeq 2$ au in H_2^+. Thus the combination of large electronic transition moments in symmetric molecules and current high laser intensities result readily in nonperturbative radiation–molecule interactions. Such effects lead to LIMPs [5–7] and charge resonant enhanced ionization (CREI), whereby molecular ionization rates can exceed that of atomic fragments by orders of magnitude at large critical internuclear distance $R_c \simeq 2R_e$, where R_e is the equilibrium distance [13–15]. Quasistatic models of atom–laser field interaction [2] have been extended to nonperturbative laser–molecule interactions with the tunneling ionization of Stark-displaced LUMOs leading to a simple consistent explanation of CREI and CE in molecules for one- or odd-electron molecular systems [13–15].

Exact numerical solution of two-electron molecules H_2 [16, 17] and H_3^+ [18], in intense laser fields in the Born–Oppenheimer approximation (static nuclei) have shown the importance of the *ionic* states, e.g., H^+H^- in H_2, predicted by Hertzberg to exist in the UV spectral region [19], as *doorway* states for CREI in these systems. Recently the ionic state of O_2, O^+O^-, has been identified by ZEKE experiments [20]. Such states have large dipole moments equal to the internuclear distance R, and thus can lead to large radiative interactions, $V(R) = ER$, exceeding molecular dissociation energies at current laser intensities. Studies of molecules in the nonlinear nonperturbative regime of molecule–radiation interaction is thus a new science requiring nonperturbative theories and numerical methods to treat laser control and manipulation of molecules in this regime [21, 22].

A seminal idea emanating from simple quasistatic models of electron ionization in atoms is the possibility of *recollision* of the ionized electron with its parent ion [3, 23]. The returning energy of the electron at the nuclei can be shown to satisfy a simple law that explains the maximum energy of harmonics emitted by such a recolliding electron,

$$N_m\hbar\omega = I_p + 3.17U_p, \tag{1}$$

where N_m is the maximum harmonic order, I_p is the ionization potential, and U_p is the ponderomotive or oscillatory energy of an electron of mass m in a pulse of frequency ω and intensity I.

$$U_p\ (\text{au}) = I/4m\omega^2 = 3.4 \times 10^{21} I(\text{W/cm}^2)\lambda^2(\text{nm}). \tag{2}$$

The corresponding field-induced displacement of such an ionized electron is given by the expression

$$\alpha\ (\text{au}) = eE/m\omega^2 = 2.4 \times 10^{-12}[I(\text{W/cm}^2)]^{1/2}\lambda^2(\text{nm}). \tag{3}$$

Thus at an intensity $I = 10^{14}$ W/cm^2 and wavelength $\lambda = 1064$ nm, $U_p = 10.5$ eV and $\alpha = 1.2$ nm. We have shown that collision of ionized electrons with neighboring ions in molecules can lead to even larger harmonic orders with photon energies of $6U_p$ up to $12U_p$, thus extending the recollision energy, cut-off law (1) [24].

Using ultrashort pulses, $t \leq 5$ fs, results in continuum HOHG in the region of the cut-off law (1) from which, by selecting a slice of the spectrum, one can synthesize *attosecond* (asec) pulses. First experimental results on the production and measurement of a 650-asec soft-X-ray pulse from high-intensity ionization of Ar atoms was reported in Refs. [25, 26]. This opens new possibilities for studying and controlling electron dynamics in atoms and molecules on asec time scales. We have recently shown that asec pulses can be used

to measure the absolute electric field of few-cycle laser pulses [27] and asec *control* of ionization and HOHG in molecules to increase HOHG intensities and thus create a new single X-ray, UV pulse as short as 250 asec [28]. We illustrate in the present paper from numerical solutions of the time-dependent Schrödinger equation (TDSE) for a 1D H_2^+ model with full electron-nuclear dynamics, i.e., from non-Born–Oppenheimer simulations, our proposed methodology for producing asec pulses from a molecular medium. Finally, we demonstrate from solutions of the TDSE how a pump-probe experiment of the photoionization of H_2^+ using asec pulses can allow one to study the evolution of the movement of localized electron wavepackets, thus leading to a new attosecond molecular spectroscopy. A pump-probe excitation of atomic states in the asec time regime has been recently demonstrated [29].

2. A Non-Born–Oppenheimer 1D TDSE for H_2^+ in Intense Laser Fields [8]

The exact 1D TDSE for H_2^+ is solved numerically describing both coupled electron (Z-coordinate) and internuclear (R-coordinate) proton coordinate by the following equation in a.u. ($\hbar = m_e = e = 1$, $m_p/m_e = 1837$, $c = 137$),

$$i\frac{\partial\psi(Z,R,t)}{\partial t} = \hat{H}(Z,R,t)\psi(Z,R,t), \tag{4}$$

where

$$\hat{H}(Z,R,t) = \hat{H}_R(R) + V_C(Z,R) + \hat{H}_Z(Z), \tag{5}$$

$$\hat{H}_Z(Z) = -\beta\frac{\partial^2}{\partial Z^2} - \kappa E(t), \quad \hat{H}_R(R) = -\frac{1}{m_p}\frac{\partial^2}{\partial R^2} + \frac{1}{R}, \tag{6}$$

$$\beta = \frac{2m_p + m_e}{4m_p + m_e}, \quad \kappa = 1 + \frac{m_e}{2m_p + m_e}, \tag{7}$$

$$V_C(Z,R) = -\frac{1}{[a + (Z \pm R/2)^2]^{1/2}}. \tag{8}$$

m_e and m_p are electron and proton masses. The Hamiltonian (5) is the exact three-body Hamiltonian obtained after separation of the center-of-mass motion, because we are working in the dipole approximation, $r/\lambda \ll 1$, where the electric field is time-dependent only [4]. The Coulomb potential is now a 1D potential requiring a softening parameter a, which is set $a = 1$ to obtain the correct I_p for H_2^+ near equilibrium. The corresponding I_p of a 1D H atom with $a = 1$ is 0.67 a.u.

The softened V_C now contains no singularity so a high-order split-operator method [30] is used to propagate the total TDSE (4) for a pulse length t_p. The integration step in space is $\delta z = 0.25$ a.u. $\sim 10^{-2}$ nm, which means that grids with $3000^2 \simeq 10^7$ points are used. The temporal time step $\delta t = 0.03$ a.u. $= 0.7$ asec so that over 1000 time steps are required for a 10-fs pulse. The electric field, $E(t)$, needs special care since such fields have total area zero [1]. Thus $E(t)$ is defined from the vector potential

$$A(t) = -cE_0(t)\sin[\omega(t - t_m) + \phi]/\omega, \tag{9}$$

$$E(t) = -(1/c)\partial A(t)/\partial t, \tag{10}$$

where $t_m = \tau/2$, i.e., half the pulse length. We generally used the pulse envelope $E_0(t)$ in the following form

$$E_0(t) = E_0\sin^2(\pi t/\tau), \quad 0 \le t \le \tau. \tag{11}$$

With $t_p = 4$ cycles $= 10.6$ fs for a 800-nm Ti:Saph laser, the pulse half-width (FWHM) is then given by $t_p = 0.3641 \simeq 4$ fs. Our definition of $E(t)$ via $A(t)$ guarantees that $A(0) = A(\tau) = E(0) = E(\tau) = 0$.

The emitted radiation spectra, constituting the HOHG spectrum in the presence of an intense laser field, can be obtained from the time-dependent acceleration for an electron in a potential $V(r)$ [31],

$$a(t) = \frac{d^2}{dt^2}\langle r\rangle = \langle\psi(t)|-\partial V/\partial r|\psi(t)\rangle. \tag{12}$$

The wave function $\psi(t)$ is the solution of TDSE (4). The Fourier transform of $a(t)$, $a(\omega)$ from which one obtains the power spectrum of HOHG $|a(\omega)|^2$, is given by

$$a(\omega) = i(2\pi)^{-1/2}e^{-i\omega\tau}\dot{d}(\tau) + i\omega e^{i\omega\tau}d(\tau) - \omega^2\int_0^\tau e^{-i\omega t}d(t)dt. \tag{13}$$

The final integral in (13) is the HOHG power spectrum using the dipole form $d(t) = \langle\psi(t)|r|\psi(t)\rangle$. Clearly, this is only valid if the transients $\dot{d}(\tau) = (d/dt)(d(t))|_{t=\tau}$ and $d(\tau)$ vanish at the end of the pulse. The accelera-

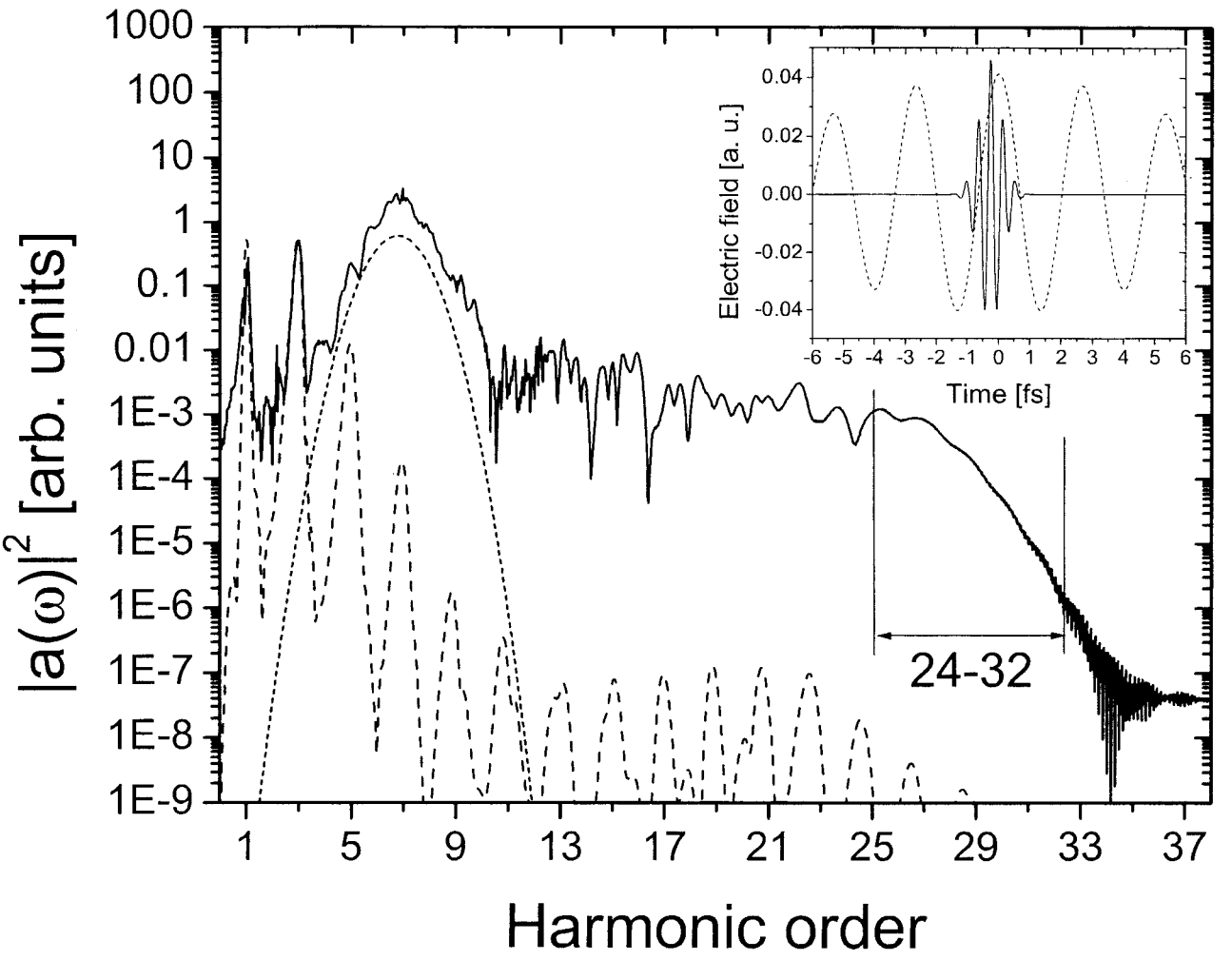

FIGURE 1. HOHG power spectrum $|a(\omega)|^2$ (arbitrary units) for non-Born–Oppenheimer H_2^+ excited by an 800-nm, 10-fs, 6×10^{13} W/cm^2 IR pulse in combination with a 600 asec (0.6-fs) 115-nm UV, probe at 2×10^{13} W/cm^2 and phase difference $\phi = \omega t = 0.1\pi$ (see inset). Solid line: fs + asec pulse excitation. Dotted line: single fs pulse excitation.

tion form emphasizes maximum acceleration, as in the case of a recolliding electron [23, 24].

This is the form we have used. Because the energy E of such an electron is $3U_p \leq E \leq 10U_p$, where U_p is the ponderomotive energy [Eq. (2)], at high intensities one has highly oscillatory electron wave functions so that the TDSE (4) requires highly accurate numerical procedures [8, 30].

3. Attosecond Pulse Synthesis

As hinted in the Introduction, one of the great advances, if not breakthroughs, emanating from research in the nonlinear, nonperturbative response of atoms to short intense laser pulses has been the synthesis of asec pulses [25, 26]. The source of asec radiation is HOHG by recollision of the ionized electron with its parent [23] or neighboring ions [24]. Unfortunately, the efficiency of such spectra is low, as illustrated in Figure 1. The dotted line represents the HOHG of H_2^+ with *moving* nuclei, i.e., non-Born–Oppenheimer, exposed in a single 10-fs 800-nm pulse with peak intensity $I = 6 \times 10^{13}$ W/cm^2. Perusal of the spectrum shows the high inefficiency of the radiation coherently emitted due to low ionization from tunneling and the uncontrolled spreading of the ionized but returning (recolliding) electron wavepacket [23, 24].

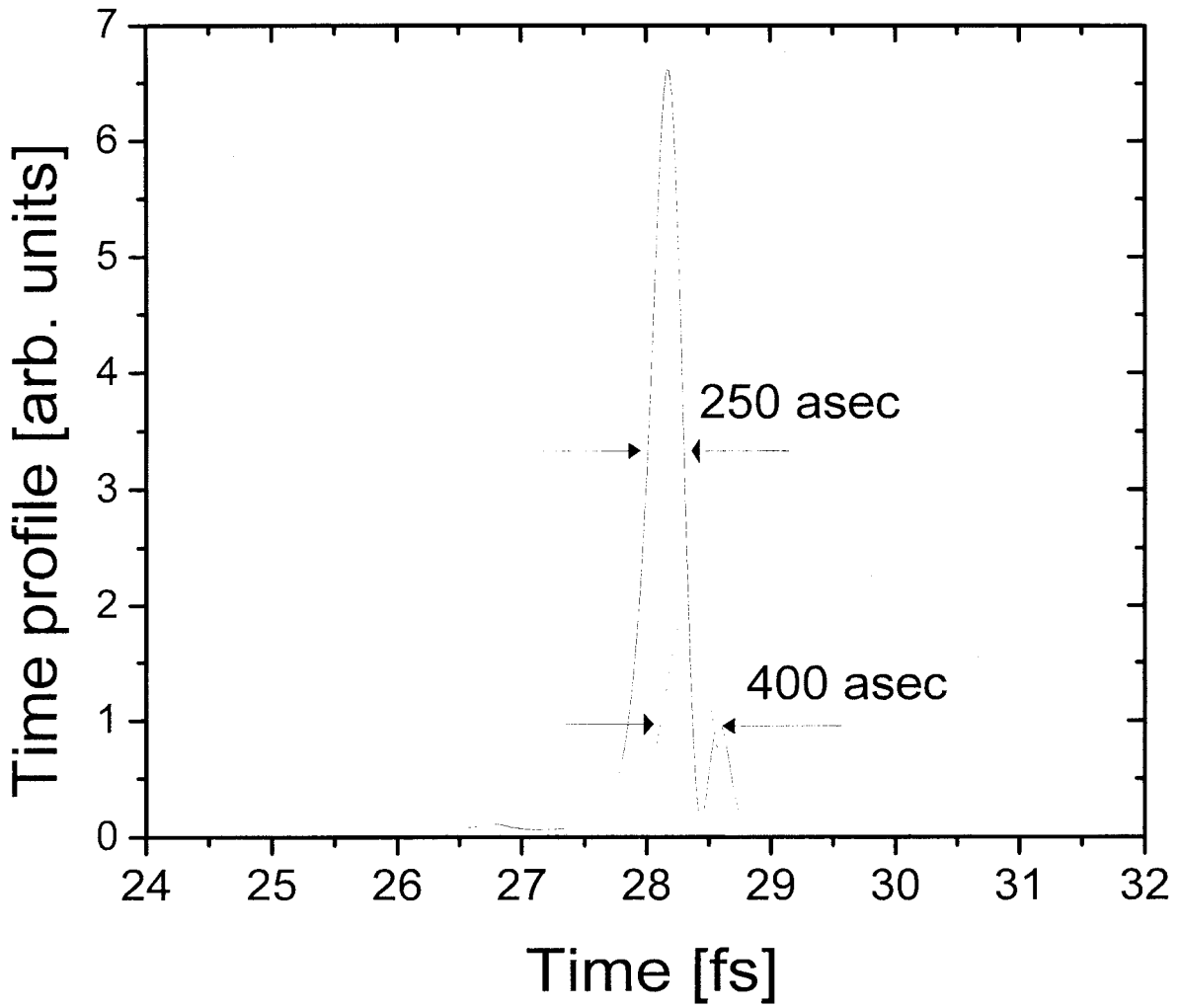

FIGURE 2. Attosecond pulses obtained from the continuous harmonics at relative phase $\phi = \omega t = -0.2\pi$ (inset Fig. 1); 400 asec from $24 < N < 32$, 250 asec from $21 < N < 32$.

To enhance such low HOHG efficiencies we originally suggested two-color excitation to preionize the electron by a high-frequency (3ω) field with subsequent control by an intense fundamental field (ω) [32]. We have recently reformulated this idea by proposing a combination of an asec VUV pulse and an intense, short 800-nm pulse [27]. The advantage of this new approach are that the *pump* asec pulse, because of its large energy bandwidth, now produces an initially narrow spatial electron wavepacket that is subsequently *controlled* by intense short (fs) low-frequency pulses. As seen in Figure 1, the HOHG spectrum is now enhanced by several orders of magnitude. The spectrum is broad and quasi-continuous near the maximum order cut-off, N_m, predicted by Eq. (1).

Such a spectrum can be used to synthesize new single UV pulses as short as 250 asec, as illustrated in Figure 2. This is obtained by combining continuous coherent radiation as an example for the order $24 \leq N \leq 32$, i.e.,

$$a(t) = \int_{24\omega}^{32\omega} a(\omega) e^{i\omega t} d\omega. \tag{14}$$

The end result is more intense asec pulses that are sensitive to the relative phase of the two colors (see inset, Fig. 1). Maximum enhancement of the new asec pulses is obtained at the relative phase $\phi = \omega t = -0.2\pi$ in contradiction to the atomic recollision

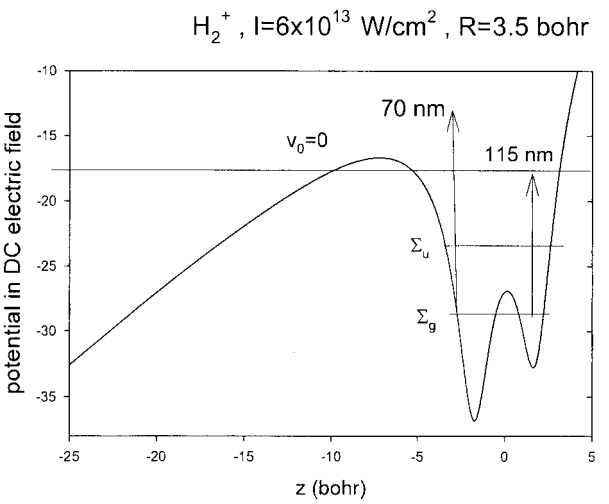

FIGURE 3. Quasistatic electronic potential $V_C(Z, R) + EZ$ at an intensity $I = cE^2/8\pi = 6 \times 10^{13}$ W/cm^2, $R = 3.5$ au for H_2^+. Applying asec pulses at $\lambda = 70$ nm and 115 nm, showing that at only $\lambda = 115$ nm creates zero velocity electrons ($v_0 = 0$) via tunneling.

model, which predicts the maximum order N_m for ionization at phase $\omega t = +0.1\pi$ with zero initial velocity due to tunneling ionization [23, 24] (see Appendix). This phase sensitivity is an extension of *coherent control* of multiphoton processes [33] into the nonlinear, nonperturbative regime of laser–molecule interaction studied in the present article.

As shown in the Appendix from simple classical mechanical considerations, zero velocity, $v_0 = 0$, electrons have maximum return energy $3.17U_p$ when ionized at phase $\phi = 0.1\pi$. It is further proved there that the electron return energy never exceeds $3.17U_p$ even when one allows for nonzero initial velocity v_0. This simple picture neglects the structure (potential) of the ion core with which the electron recollides. In particular for H_2^+ (Fig. 3) one sees that the electron ionized at 115 nm is different from that at 70-nm wavelength. Thus, at 115 nm, the electron must tunnel out to ionize via the static Coulomb barrier, $V_C(Z, R) + EZ$, and thus leave with zero velocity, $v_0 = 0$, at the outer turning point. However, the presence of the intense (6×10^{13} W/cm^2) 800-nm prepulse traps the initial (Σ_g) electron wavepacket in the lower left well. The 115-nm asec pulse thus creates an electron wavepacket localized near the maximum on the left of the distorted double well. This wavepacket can recross the whole molecule from left to right and ionize after reflection from the right well. It will exit and produce maximum ionization when the barrier on the left is minimum. This is achieved by the electron wavepacket being prepared at initial lower field phase, $\omega t = -0.2\pi$, so that on recrossing the whole molecule and then exiting the barrier is lowest at $\omega t = 0$, i.e., at the maximum of the field. This simple explanation emphasizes the importance of the potential of the ion core on the phase sensitivity of harmonic generation in H_2^+.

4. Electron Localization

In the previous section we showed how the molecular ion H_2^+ can be used to create intense sub-fs or equivalently asec pulses in the VUV frequency (wavelength) region. Thus, as shown in Figures 1 and 2, combining harmonics by filtering techniques [25] between the 24th and 32nd will create sub-fs pulses with considerable bandwidth. Here we examine the broadband electronic excitation of H_2^+ at fixed internuclear distance $R = 8$ au, which is excited by an 800-asec (0.8-fs) 115-nm *pump* pulse followed by a 100-asec (0.1-fs) 20-nm *probe* pulse (Fig. 4). The latter induces direct one-photon ionization, and we use the corresponding photoelectron spectrum to monitor the subsequent electron motion. All calculations were performed using the numerical code to solve the TDSE equation (4) but with nuclei fixed at $R = 8$ au, because the pulses are much shorter than the typical H atom motion time of ~10 fs. The TDSE thus yields the exact electronic wave function $\psi(Z, t)$, from which one can calculate the induce dipole moment $d(t) = \langle\psi(Z, t)|Z|\psi(Z, t)\rangle$.

Excitation at 50 nm shows that the induced dipole (Fig. 4) is completely in phase with the field $E(t)$, since such short wavelengths ionize the electron which then follows the field. At 115 nm, which corresponds nearly to the H atom 1s–2p transition, one observes that the dipole is out of phase with $E(t)$ but shows a periodic oscillation of 0.35 fs or equivalently a photon energy at 105 nm ($\lambda = \tau c$). The dipole oscillations resulting from 150-nm, 800-asec excitations are much more reduced in intensity. The obvious explanation is that, at 115-nm excitation, one is exciting electronic states by transition to $2\sigma_u$ orbitals and others formed from $2s$ and/or $2p\sigma$ atomic orbitals of H, whereas at 150 nm one is below such resonances and the induced dipole is much reduced. Thus, the resulting electronic wave function can be represented as the combination

$$\psi(t) = c_1(t)\psi_{1\sigma_g} + c_2(t)\psi_{2\sigma_u}. \qquad (15)$$

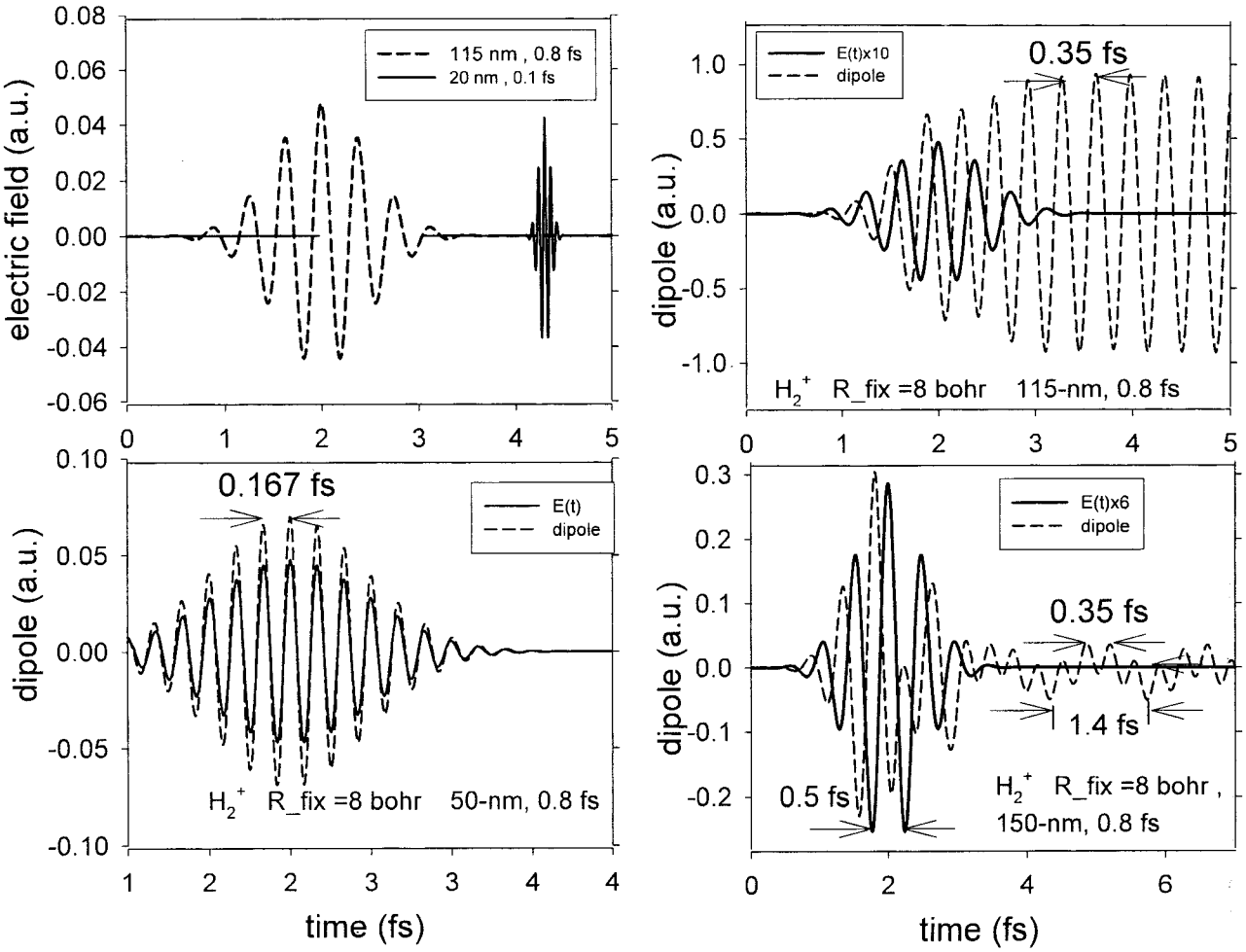

FIGURE 4. Resulting induced dipoles in arbitrary units for H_2^+ at $R = 8$ au excited by 50-nm, 115-nm, 150-nm, 0.8-fs (800-asec) pulses.

The corresponding induced dipole can be readily calculated to be

$$d(t) = \langle\psi(t)|Z|\psi(t)\rangle = c_1(t)c_2^*(t)\langle 1\sigma_g|Z|2\sigma_u\rangle e^{i(E_1-E_2)t} + \text{c.c.}, \quad (16)$$

which oscillates at the frequency corresponding to the energy difference $E_1 - E_2$ between the ground $1\sigma_g$ and excited $2\sigma_u$ molecular orbitals at $R = 8$ au. Furthermore, since $1\sigma_g \simeq (1/\sqrt{2})[1s_a + 1s_b]$ and $2\sigma_u \simeq (1/\sqrt{2})[2p\sigma_a - 2p\sigma_b]$ have the largest dipole $\langle 1\sigma_g|Z|2\sigma_u\rangle \simeq \langle 1s|Z|2p\sigma\rangle$, then the resulting time-dependent wave function $\psi(t)$ is an sp hybrid ($1s \pm 2p\sigma$) situated on each proton. This laser-induced hybridization is clearly evident in Figure 5 where we illustrate the electron density $|\psi(Z; t)|^2$ as a function of time. One see initially that the electron is delocalized equally between the two protons at $Z = \pm 4$ au. After excitation with an 0.8-fs, 115-nm pulse one sees the electron density polarized inside the molecular bond, toward $Z = 0$ corresponding to a single sp hybrid, i.e., $s + p$, which oscillates between the two nuclei with the period of the energy difference $E_1 - E_2 = 0.35$ fs or 350 asec. Because this oscillation is an induced dipole corresponding to oscillation from H^+H to HH^+ electronic configurations, emitted radiation will occur at the wavelength 105 nm. However, this will give no indication of the position of the electron.

We therefore propose here a spectroscopic method of spatially locating the electron. This is based on the resulting ionization asymmetry predicted from ionization by intense ultrashort pulses and used to measure the electric field phase profile

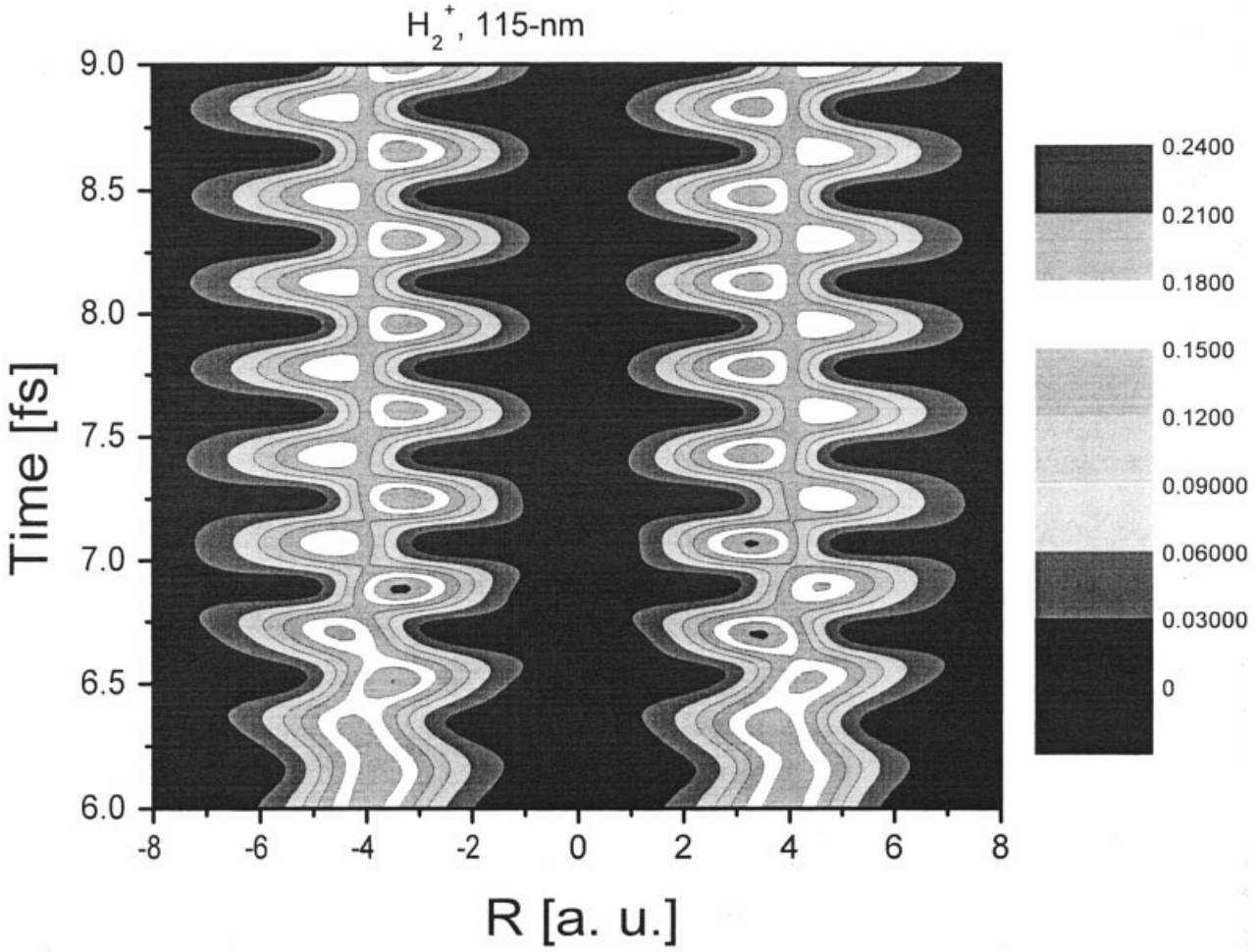

FIGURE 5. Electron probability $|\psi(Z, t)|^2$ at $R = 8$ au following excitation at 115-nm with 0.8-fs pulse (see Fig. 4).

of such pulses by asec probe pulses [27]. Thus, as shown in Figure 4, a 20-nm, 100-asec pulse is used to ionize the sp hybrids prepared by the 115-nm, 800-asec prepulse. As illustrated in Figure 6, the resulting ionization asymmetry is defined as

$$P_2/P_1 = \frac{P_- - P_+}{P_- + P_+}, \tag{17}$$

where $P_{-(+)}$ is the left (right) ionization probability collected at opposing directions. This asymmetry pulsates precisely with the frequency corresponding to the energy difference, $E_1 - E_2$, between the ground and excited states that are coherently excited by the first (115-nm) asec pulse. Figure 5 demonstrates that the asymmetry oscillations correspond to transfer of a localized electron between the different protons.

5. Conclusion

We have shown from solution of the TDSE for H_2^+ that we can generate efficiently new ultrashort, asec, pulses by the combination of a previously obtained asec probe with an intense short IR pulse such as a 10-fs, 800-nm Ti:Saph pulse. Such asec pulses can be used to create localized electron wavepackets in molecules which oscillate between nuclei on these asec time scales. Measuring the directional photoelectron spectrum of such wavepackets or hybrids produces ionization asymmetries which follow the electon position in the molecule on asec time scales. We have recently proposed asymmetric ionization as a new tool for measuring the absolute phase of ultrashort (~asec) pulses [34]. Asec time resolu-

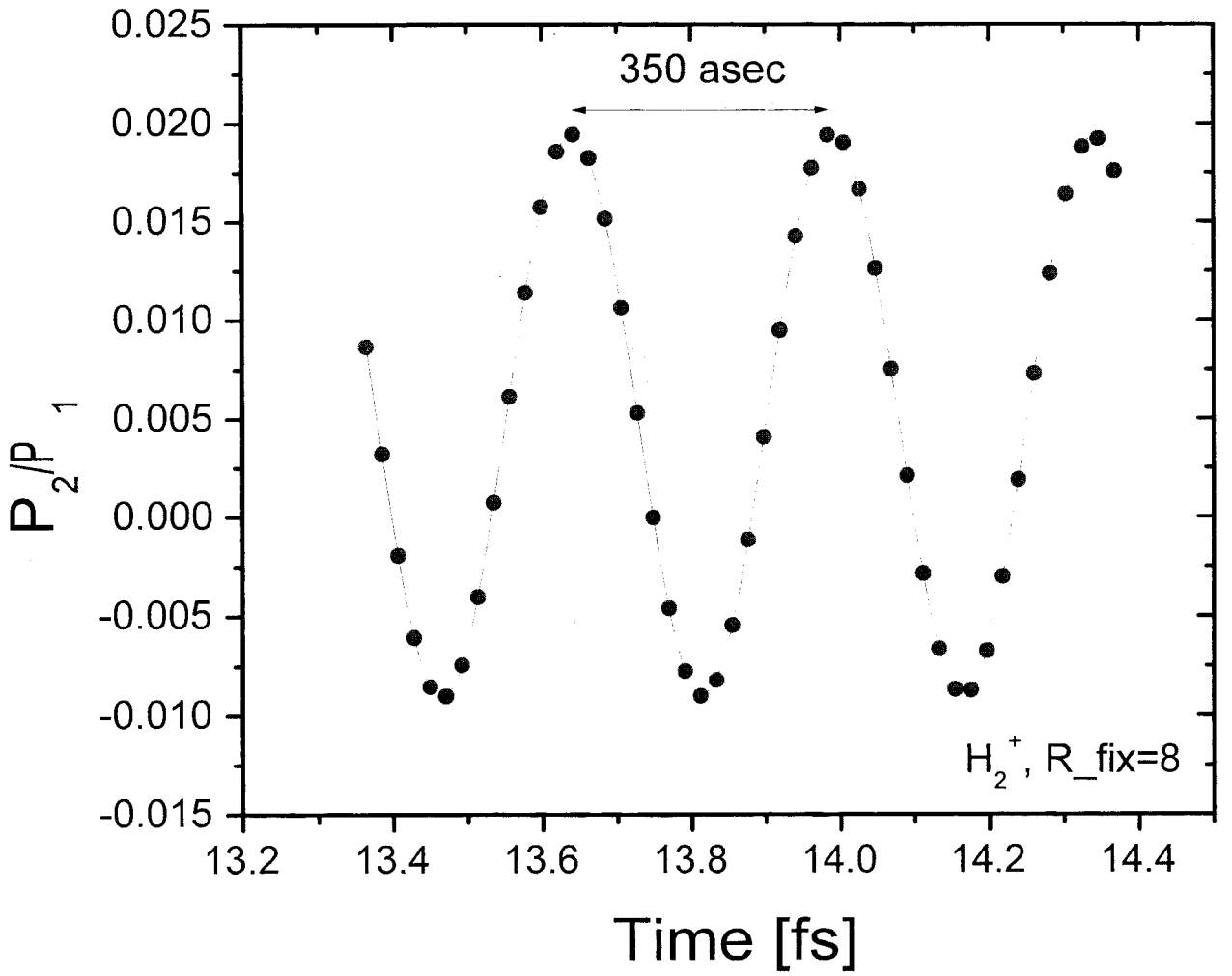

FIGURE 6. Asymmetry in the ionization yield, P_2/P_1 [Eq. (17)], of the directional photoelectron spectrum of the electron distributions (Fig. 5) as a function of time delay between a 20-nm, 0.1-fs (100-asec) ionization pulse.

tion of such ionization is a new experimental challenge.

ACKNOWLEDGMENT

We thank Paul Corkum (NRC, Ottawa) and Ferencz Krausz (Vienna) for "illuminating" discussions on asec pulse metrology.

References

1. Brabec, T.; Krausz, F. Rev Mod Phys 2000, 72, 545.
2. Gavrila, M. Atoms in Intense Laser Fields, Academic Press: New York, 1992.
3. Krause, J. L.; Schafer, K. J.; Kulander, K. Phys Rev Lett 1992, 68, 3535.
4. Bandrauk, A. D. Molecules in Laser Fields; M. Dekker: New York, 1994.
5. Bandrauk, A. D.; Sink, M. L. J Chem Phys 1981, 74, 1110; Chem Phys Lett 1978, 57, 569.
6. Wunderlich, C.; Kohler, E.; Figger, H.; Hansch, T. Phys Rev Lett 1997, 78, 2333.
7. Pavicic, D.; Figger, H.; Hansch, T. Eur Phys J 2003, D26, 39.
8. Chelkowski, S.; Foisy, C.; Bandrauk, A. D. Phys Rev 1998, A57, 1156.
9. Kawata, I.; Bandrauk, A. D. Phys Rev 2003, A67, 013407.
10. Chelkowski, S.; Corkum, P. B.; Bandrauk, A. D. Phys Rev Lett 1999, 82, 3416.
11. Bandrauk, A. D.; Chelkowski, S. Phys Rev Lett 2002, 87, 273004.
12. Mulliken, R. S. J Chem Phys 1939, 7, 20.

13. Zuo, T.; Bandrauk, A. D. Phys Rev A 1995, 52, 2511; 1996, 54, 3254.
14. Seideman, T.; Ivanov, M. Y.; Corkum, P. B. Phys Rev Lett 1995, 75, 2819.
15. Chelkowski, S.; Bandrauk, A. D. J Phys B 1995, 28, L723.
16. Kawata, I.; Kono, H.; Bandrauk, A. D. Phys Rev A 2000, 62, 031401.
17. Harumiya, K.; Kono, H.; Bandrauk, A. D. Phys Rev A 2002, 66, 043403.
18. Kawata, I.; Kono, H.; Bandrauk, A. D. Phys Rev A 2001, 64, 043911.
19. Herzberg, G. Spectra of Diatomic Molecules; Van Norstrand: New York, 1951.
20. Martin, J. D.; Hepburn, J. W. Phys Rev Lett 1997, 79, 3154.
21. Laser Control and Manipulation of Molecules; Bandrauk, A. D.; Fujimura, Y.; Gordon, R. J., Eds.; ACS Symposium Series 821; American Chemical Society: Washington, DC, 2002.
22. Quantum Control; Bandrauk, A. D.; Delfour, M.; Le Bris, C., Eds.; CRM Proceedings and Lecture Notes, Vol. 33; American Mathematical Society: Providence, RI, 2003.
23. Corkum, P. B. Phys Rev Lett 1993, 71, 1994.
24. Bandrauk, A. D.; Yu, H. Phys Rev A 1999, 59, 539; J Phys B 1998, 31, 4243.
25. Hentschel, M.; Kienberger, R.; Spielmann, C.; Reider, G.; Milosevic, N.; Brabec, T.; Corkum, P.; Heinzmann, U.; Drescher, M.; Krausz, F. Nature (London) 2001, 414, 509.
26. Kleineberg, U.; Heinzmann, U.; Drescher, M.; Krausz, F. Science 2002, 297, 1144.
27. Bandrauk, A. D.; Chelkowski, S.; Nguyen, H. S. Phys Rev Lett 2002, 89, 283903.
28. Bandrauk, A. D.; Nguyen, H. S. Phys Rev A 2002, 66, 031401.
29. Kienberger, R.; Baltuska, A.; Yakovlev, V.; Scrinzi, A.; Drescher, M.; Krausz, F. Nature 2004, 427, 817.
30. Bandrauk, A. D.; Shen, H. J Chem Phys 1993, 99, 1185.
31. Jackson, J. D. Classical Electrodynamics; Wiley: New York, 1962.
32. Bandrauk, A. D.; Chelkowski, S.; Yu, H.; Constant, E. Phys Rev A 1997, 56, 2357.
33. Shapiro, M.; Brumer, P. Principles of the Quantum Control of Molecular Processes; Wiley Interscience: New York, 2002.
34. Chelkowski, S.; Bandrauk, A. D.; Apolonski, A. Phys Rev A 2004, to appear.

Appendix

We solve the classical equation of motion of an electron in a laser field $E(t)$:

$$\frac{d^2z}{dt^2} = \frac{dv}{dt} = -E_0\cos(\omega t), \quad v(t_0) = v_0, \quad z(t_0) = z_0 = 0. \tag{A.1}$$

Its solution is

$$v(t_f) = v_0 + X\sin(\phi_0) - X\sin(\phi_f) \tag{A.2}$$

$$z(t_f) = [v_0 + X\sin(\phi_0)](\phi_f - \phi_0)/\omega + \frac{X}{\omega}[\cos(\phi_f) - \cos(\phi_0)], \tag{A.3}$$

where $X = E_0/\omega$, $\phi_0 = \omega t_0$, $\phi_f = \omega t_f$. The final velocity is maximum (for $v_0 > 0$) when $\phi_0 = \pi/2$ and $\phi_f = 3\pi/2$, then it is equal to $v_t = v_0 + 2X$. If $v_0 = 0$, the maximum energy is

$$v_f^2/2 = 2 \times X^2 = 8U_p, \tag{A.4}$$

where $U_p = X^2/4$ is the ponderomotive energy. This maximum energy can be reached only at $z \neq 0$, [24], when

$$|z(t_f)| = \frac{E_0}{\omega^2}(2n-1)\pi, \quad \text{with } n = 1, 2, \ldots. \tag{A.5}$$

It was previously shown [3, 23, 24] that if the electron initial velocity is $v_0 = 0$, then the maximum energy that the electron can acquire at its return [i.e., when $z(t_f) = 0$] is $E_f = v_f^2/2 = 3.17314U_p$. We show that this result is also valid for the nonzero initial velocity v_0, i.e., we show that allowing a nonzero initial velocity v_0 leads to the same maximum energy of the electron at its return, i.e., to $E_f = 3.17314U_p$, which occurs at $v_0 = 0$.

We impose the condition of the electron return $z(t_f) = 0$; thus using Eq. (A.3), we can express v_0 as a function of ϕ_0, ϕ_f, or (as appears to be more convenient), as a function of ϕ_0, $\Delta = \phi_0 - \phi_f$ (which is the relative phase between the initial and final times):

$$\frac{v_0}{X} = \beta_1\cos(\phi_0) + \beta_2\sin(\phi_0),$$

$$\beta_1 = \frac{1-\cos(\Delta)}{\Delta}, \beta_2 = \frac{\sin(\Delta)}{\Delta} - 1. \tag{A.6}$$

After inserting (A.6) into (A.2) we get the following expression for the electron velocity at the return time:

$$\frac{v_f}{X} = f(\Delta, \phi_0) = \alpha_1\cos(\phi_0) + \alpha_2\sin(\phi_0),$$

$$\alpha_1 = \frac{1-\cos(\Delta)}{\Delta} - \sin(\Delta), \quad \alpha_2 = \frac{\sin(\Delta)}{\Delta} - \cos(\Delta). \tag{A.7}$$

Equation (A.7) gives all possible return velocity with *nonzero* v_0. For any value of Δ, ϕ_f, v_0 can be

calculated from (A.6). We note that $v_f/X = f(\Delta, \phi_f)$ is the function of two independent variables Δ, ϕ_f. We find extrema of $f(\Delta, \phi_f)$ by requiring its partial derivatives to be zero, which leads us to the two equations determining the coordinates of the extrema of the function $f(\Delta, \phi_f)$:

$$\frac{\partial f}{\partial \Delta} = \alpha_1' \cos(\phi_0) + \alpha_2' \sin(\phi_0) = 0, \quad \text{(A.8)}$$

$$\frac{\partial f}{\partial \phi_0} = -\alpha_1 \sin(\phi_0) + \alpha_2 \cos(\phi_0) = 0, \quad \text{(A.9)}$$

where α_1' and α_2' are derivatives of $\alpha_1(\Delta)$ and $\alpha_2(\Delta)$. After elimination of ϕ_0 from (A.8), we get from (A.7) the following equation determining Δ:

$$F(\Delta) = 2 - 2\sin(\Delta) + \cos(\Delta)(\Delta^2 - 2) = 0. \quad \text{(A.10)}$$

The function $F(\Delta)$ has the following zeroes: $\Delta_1 = 1.30048\pi$, $\Delta_2 = 2.4265\pi$, $\Delta_3 = 3.435\pi$, $\Delta_4 = 4.458\pi$, $\Delta_5 = 5.461\pi, \ldots$. To each of these values, using (A.9), we find following ϕ_0's [using the relation $\phi_0 = \arctan(\alpha_2/\alpha_1)$]: 0.097607π, 0.0367498π, 0.032395π, 0.02079π, 0.0193425π. The first corresponds to the maximum value of $v_f = 1.2595905X$, i.e., to the kinetic energy at the electron return: $v_f^2/2 = 3.1731365668U_p$; all next extrema correspond to lower energies: $1.5423U_p$, $2.4043U_p$, $1.734U_p$, $2.246U_p$. At all of them, v_0 is zero, as we show below. For large Δ the final velocity simplifies to

$$\frac{v_f}{X} = f(\Delta, \phi_0) \simeq -\sin(\Delta + \phi_0) = -\sin(\phi_f), \text{ for } \Delta \gg 1. \quad \text{(A.11)}$$

This means that for large delays, $\Delta \gg 1$, the final kinetic energy at the electron return to $z = 0$ never exceeds $2U_p$. Thus we have proved that the electron final energy at the electron return *never exceeds* $3.173137U_p$, even when one allows the nonzero initial velocity v_0.

Next we show that v_0 is 0 at any extrema of the function $v_f/X = f(\Delta, \phi_0)$, defined by $\partial f/\partial\phi_0 = \partial f/\partial\Delta = 0$. First, we find from (A.9) that $\tan(\phi_0) = \alpha_2/\alpha_1$. Next, we insert it into (A.6) and get:

$$\frac{v_0}{X} = \cos(\phi_0)\left[\frac{1-\cos(\Delta)}{\Delta} + \left(\frac{\sin(\Delta)}{\Delta} - 1\right)\frac{\alpha_2}{\alpha_1}\right] = \frac{\cos(\phi_0)}{\alpha_1 \Delta^2} F(\Delta). \quad \text{(A.12)}$$

Note that v_0 is proportional to $F(\Delta)$; therefore we conclude from (A.10) that at any extremum of the function $f(\Delta, \phi_0)$, v_0 is zero. In other words, we have proven that the highest energies at the electron return occur when $v_0 = 0$.

Similarly, to find the maximum possible initial velocity v_0, we seek extrema of function $h(\Delta, \phi_0) = v_0/X$:

$$\frac{\partial h}{\partial \Delta} = \beta_1' \cos(\phi_0) + \beta_2' \sin(\phi_0) = 0, \quad \text{(A.13)}$$

$$\frac{\partial h}{\partial \phi_0} = \beta_1 \sin(\phi_0) + \beta_2 \cos(\phi_0) = 0. \quad \text{(A.14)}$$

These conditions lead to $F(\Delta) = 0$ [see Eq. (A.10)], i.e., to the same condition as in the case of the extrema of v_f/X. Thus extrema of the function $h(\Delta, \phi_0)$ occur at some value of Δ: $\Delta_1, \Delta_2, \ldots$, as in the case of v_f, but at different ϕ_0 values, which can be calculated from (A.14)

$$\phi_0 = \arctan(\beta_2(\Delta)/\beta_1(\Delta)). \quad \text{(A.15)}$$

We list below the values of Δ_i obtained from (A.10) and in the next line the corresponding values of ϕ_0 obtained with the help of (A.15), followed by the corresponding values of v_0/X:

Δ:	1.30048π,	2.4265π,	3.435π,	4.458π,	5.461π
ϕ_0:	-0.40024π,	-0.46325π,	-0.476π,	-0.4788π,	-0.4803π
v_0/X:	1.25959,	0.87815,	1.09642,	0.931285,	1.05987

We conclude that we have always

$$|v_0| < v_{\max} = 1.1295905X = 1.1295905E_0/\omega. \quad \text{(A.16)}$$

In other words, if we initialize the classical trajectory with the initial velocity exceeding $v_{\max}$, *the electron will never return* to its starting point, $z = 0$ (this is true for all possible initial phases ϕ_0), and, consequently, no harmonic generation occurs for high initial velocity $|v_0|$.